Metal vapor lasers. Applications to atmospheric optics studies

G.S. Evtushenko and V.M. Klimkin

Institute of Atmospheric Optics,
Siberian Branch of the Russian Academy of Sciences, Tomsk

Received July 1, 1999

A review of modern applications of metal vapor lasers (MVL's) to atmospheric optics studies is presented, as well as some examples of MVL use in single-frequency and multifrequency sounding devices and visual navigation systems. A capability is demonstrated of using MVL's as sources of coherent radiation in solving problems of radiation propagation through dense scattering media, as well as in spectroscopy of atmospheric gases, diagnostics of iodine radionuclides, detection and ranging of metal vapor layers, and creation of "artificial" reference stars in the upper atmospheric layers.

1. Introduction

One of the promising applications of metal vapor lasers (MVL's) is atmospheric optics: spectroscopy and gas analysis of atmospheric and foreign gases, radiation propagation and remote sensing of the atmosphere to determine its thermodynamic, meteorological, and optical parameters. Requirements imposed on the MVL's as sources of coherent radiation for atmospheric optics devices were considered in Ref. 1.

2. MVL's in remote sensing

The methods of laser sounding of atmospheric composition and dynamic processes providing for real-time monitoring of the atmosphere are based on recording of echo signals from laser pulses emitted into the atmosphere. The atmosphere in this case is considered as a scattering and absorbing medium. Let us consider a receiving system with the area S and a transmitter capable of sending pulses of power P_0 and duration τ at a wavelength λ. Then the power of the recorded optical signal from a scattering volume at the distance R from the transceiver is described by the lidar equation

$$P(\lambda, R) = k P_0 \frac{c\tau}{2} \frac{S}{R^2} \beta_\pi(\lambda, R) \times \times \exp\left[-2 \int_0^R \alpha(\lambda, r)\, dr \right], \quad (1)$$

where k is the efficiency of the transceiver; c is the speed of light; $\beta_\pi(\lambda, R)$ is the volume backscattering coefficient; $\alpha(\lambda)$ is the volume extinction coefficient of the medium at the laser radiation wavelength.

Equation (1) is to be solved to obtain the profiles of α and β_π along the sounding path and to assign them a physical meaning. Mathematically this problem is an ill-posed problem and requires special methods for solution and, correspondingly, some simplifying assumptions.[3] Since the parameters α and β depend on λ, the use of a laser emitter operating simultaneously at different wavelengths allows one to write down a set of equations of the type of Eq. (1) for different λ and to determine the profile, size, nature, and concentration of scattering (or absorbing) particles.

Single-frequency sounding allows reconstruction of the profile of the extinction coefficient and (provided that some *a priori* information is available) estimation of the aerosol density profile. At the same time, multifrequency sounding allows determination of not only density profiles, but also concentration of aerosol particles, their size, and nature, as well as concentration of ozone in the troposphere and stratosphere.[4–6] The method based on the effect of spontaneous Raman scattering of light by molecules of atmospheric and foreign gases enables one to write a set of equations of the type of Eq. (1) for signals at the basic and Raman frequencies and to determine the altitude profiles of air temperature, humidity, and wind velocity. Sounding along slant and horizontal paths provides a possibility of monitoring the atmosphere to identify the character and concentrations of atmospheric pollutants.[7–9]

2.1. MVL in application to single-frequency sounding

Figure 1*a* shows the results of single-frequency sounding of industrial aerosol along a horizontal path over the industrial area of Tomsk. The copper vapor repetitively pulsed laser with the mean output power of 1 W at the basic wavelength (510.6 nm) was used as a source of laser radiation.[10] Here $P^*(R)$ is the scattering ratio:

$$P^*(R) = [\beta_a(R) + \beta_m(R)]/\beta_m(R), \quad (2)$$

where $\beta_a(R)$ and $\beta_m(R)$ are the aerosol and molecular backscattering coefficients; R is the distance.

0235-6880/99/09 840-09 $02.00

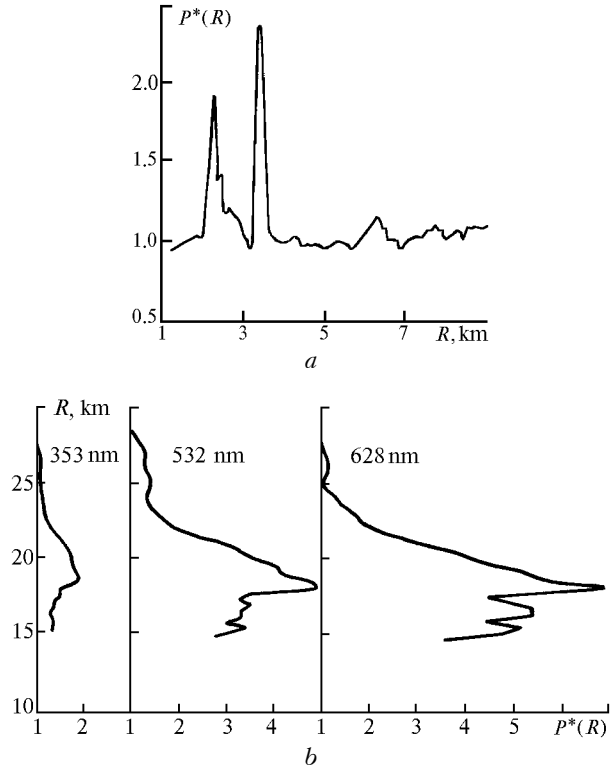

Fig. 1. Some results of aerosol sounding with metal vapor lasers: horizontal profile of the scattering ratio at the Cu-vapor laser wavelength λ = 510 nm (*a*); vertical profiles of the scattering ratio at three wavelengths (628 nm of the Au-vapor laser) (*b*).

The scattering ratio $P^*(R)$ characterizes relative contribution of aerosol (mostly, industrial) and molecular components to the lidar return signal. Spikes of the aerosol signal at the distance of 2.5, 3.5, and 6.5 km well correlate with the positions of industrial objects and smoke plumes along the sounding path. Unfortunately, the obtained data do not allow one to judge on the character of pollution and pollutant concentration. Such a lidar system based on copper and Au vapor lasers was used in research carried out by Bulgarian scientists[11] to measure the profiles of aerosol distribution in the troposphere and stratosphere.

The method employing the effect of Raman scattering was applied at the Institute of Atmospheric Optics by Arshinov et al.[7] in a copper-vapor-laser-based lidar. The lidar was designed for obtaining the information on content of gaseous constituents, temperature and humidity profiles, as well as wind speed and velocity in the surface atmospheric layer (several kilometers thick). For the years elapsed from construction of the first version of the Raman lidar with a copper-vapor laser, several modifications of this lidar have been designed: from a stationary to mobile device.[5–7] Figure 2*a* borrowed from Ref. 7 demonstrates two temperature profiles first obtained by the lidar method (dots) in comparison with the data of balloon-borne measurements (solid curves).

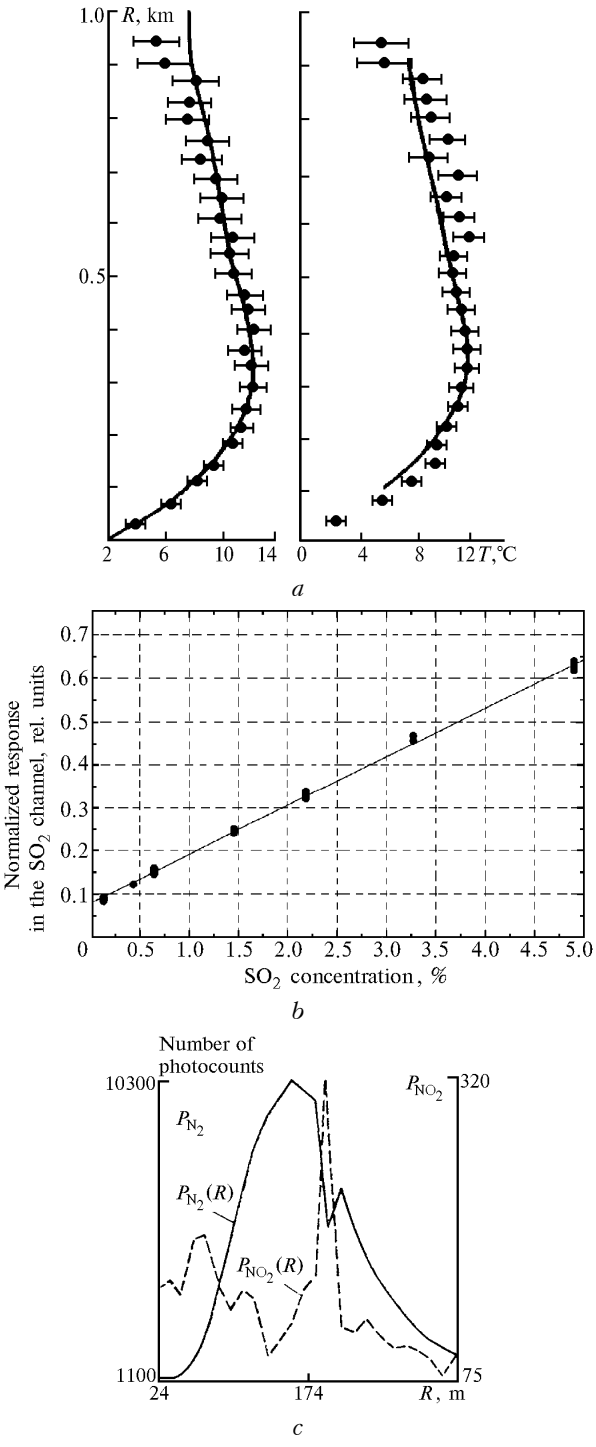

Fig. 2. Capabilities of Raman lidar with a copper-vapor laser (λ = 510.6 nm): altitude profiles of the air temperature in the atmosphere (*a*); normalized (against nitrogen) lidar responses vs. the SO_2 concentration (model experiment) (*b*); actually observed lidar signals (number of photocounts) from the nitrogen (P_{N_2}) and nitrogen dioxide (P_{NO_2}) molecules along the sounding path across the smoke stack of a coke baking battery.

Figures 2*b* and *c* (borrowed from Refs. 8 and 9) illustrate the capabilities of the Raman lidar as applied

to the problem of detecting gaseous pollutants. The pollutant density is determined from the ratio of the Raman lidar signal backscattered from the pollutant to the simultaneously recorded signal from nitrogen. Since the nitrogen concentration in the atmosphere can be considered known, the change in the ratio between the above-indicated signals is proportional to the concentration of a pollutant.

2.2. MVL as applied to multifrequency scattering

For complex study of the processes of weather and climate formation and for monitoring the general ecological situation over industrial regions, a complex lidar station has been designed at the Institute of Atmospheric Optics. The lidar station includes the main mirror of 2.2-m diameter and a set of laser emitters including Cu-, Au-, and Pb-vapor lasers, among them the lasers with frequency conversion in nonlinear crystals and dyes.[10]

Figure 1*b* shows the results of simultaneous sounding of the atmosphere at three wavelengths, including the basic wavelength of the Au-vapor laser (627.8 nm). These results were obtained by Burlakov et al. (Laboratory of Remote Spectroscopy of the Atmosphere, IAO SB RAS) in spring 1992 (Ref. 10). The altitude profiles of the scattering ratio $P^*(R)$, where R is the altitude, present the aerosol situation characteristic of that time in the Western-Siberian region. This situation was caused by the aerosol perturbation of the atmosphere by the products of Mt. Pinatubo eruption which occurred in summer 1991 at the Philippines. The data obtained in these experiments were used for aerosol correction of the measurements of the altitude profiles of ozone derived from differential absorption at the wavelengths of 308 nm (XeCl laser) and 353 nm (third harmonic of the Nd–YAG-laser).

The MVL radiation can also be used to obtain the ozone profiles by DIAL method. As an example, Fig. 3*a* shows the results of numerical simulation of the tropospheric ozone sounding by the DIAL method[12] at the frequencies of the copper vapor laser converted in a BBO crystal (wavelengths of 255, 271, and 289 nm fall within the Hartley–Higgins absorption band of the ozone molecule). The sounding altitude is plotted as an ordinate, and the total error in determination of the ozone density is plotted as an abscissa. This error is caused by the instrumental errors, background radiation, light absorption by water vapor and other gases in this spectral region. Figure 3*b* shows the experimentally recorded echoes at the mean power of the converted radiation of 0.5 W (at the 255, 271, and 289 nm UV lines) and the pulse repetition rate of 7 kHz (Ref. 13). The data obtained indicate that by using a pair of lines (271 and 289 nm) near the maximum of the ozone absorption band and at the wing of the Hartley–Higgins band, reliable monitoring of ozone is possible at the altitude ranging from 2 to 5 km in daytime and from 2 to 6 km at night with the signal accumulation time of 10 min (in the photon counting mode). Another pair of lines (255 and 271 nm) is worse for ozone sounding in the troposphere, because the 255-nm line lies at the maximum of the ozone absorption band and is strongly absorbed in the near ground layer of the atmosphere. Correspondingly, this pair better fits the ozone sounding along horizontal near-surface paths.

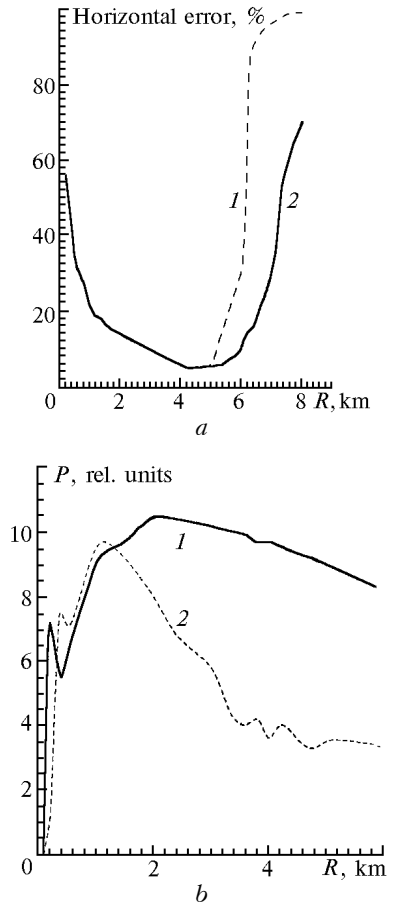

Fig. 3. Capabilities of the UV laser system (Cu-vapor laser + ""O crystal) for sounding of the tropospheric ozone: the upper panel shows the results of simulation for day (curve *1*) and night (curve *2*); the lower panel shows the experimental results at $\lambda = 289$ nm (curve *1*) and $\lambda = 271$ nm (curve *2*), $P = \ln (R^2 \times \text{signal})$.

The above-mentioned spectral dependence of the backscattering coefficient can be used for estimating the microstructure characteristics of aerosol.[5,6] Metal vapor lasers operating at transitions in a wide spectral region from the UV to near IR are promising for solution of such problems. They can guarantee high spatial and temporal resolution. An example of qualitative interpretation of the data of multifrequency

sounding with the Cu–Au mixture vapor laser (λ = 510.6, 578.2, and 627.8 nm) can be found in Ref. 14. Reliable quantitative data can be obtained by using a larger number of MVL lasing lines in a wide spectral region, where the spectral behavior of the backscattering coefficient differs more markedly. In particular, highly effective Pb (722.9 nm) and barium (1.13 and 1.15 μm) vapor lasers or laser operating on a mixture of vapors of these elements can be used in addition to the above-mentioned lasers.[1]

However, one should keep in mind that high repetition rate of laser pulses f restricts the range of lidar systems because of the overlap of signals from two or more successively emitted pulses ($R < cf/2$, where c is the speed of light). Thus, for the sounding altitudes above 15 km, the pulse repetition rate should be less than 10 kHz, and for the altitude above 60 km it should be less than 2.5 kHz. Then, relatively low energy per pulse significantly restricts the lidar range under conditions of background illumination (for example, in daytime measurements). However, the range can be increased using a monoisotopic laser and interferometer as a spectral selector of a lidar.

3. MVL's in the UV spectroscopy of the atmosphere

In Ref. 15 the diagnostic system based on the copper vapor laser with frequency conversion in the nonlinear BBO crystal and opto-acoustic detector was applied to recording the water vapor absorption in the UV spectral region. The absorption band found in Ref. 16 lies in the 250–320 nm spectral region, and the knowledge of the absorption coefficient is of principal importance for lidar determination of concentrations of some minor atmospheric constituents, in particular, ozone (see Section 2.2). The data available by then on the absorption coefficient[16–18] measured by the fluorescent and spectrophotometric methods differed markedly: from 10^{-8} to 10^{-9} $cm^{-1}\cdot Pa^{-1}$. Figure 4 shows the signals of the opto-acoustic detector excited by the radiation (255, 271, and 289 nm) as its working chamber is filled with pure nitrogen and water vapor mixed with the nitrogen buffer gas at different pressures. Note that differences in opto-acoustic signals in pure nitrogen and the mixture of N_2 with water vapor are significant and most likely are caused by water vapor absorption of UV radiation. The absorption coefficients for the m_2n-N_2 binary mixture estimated from the tilt of the curves in Fig. 4*a* were: $2.3\cdot10^{-9}$ (for the 255 nm wavelength), $0.9\cdot10^{-9}$ (271 nm), and $1.6\cdot10^{-9}$ $cm^{-1}\cdot Pa^{-1}$ (289 nm), what correlates with the data from Ref. 14. The observed wavelength dependence of the absorption coefficient is very interesting, but additional experiments are needed for serious conclusions to be drawn.

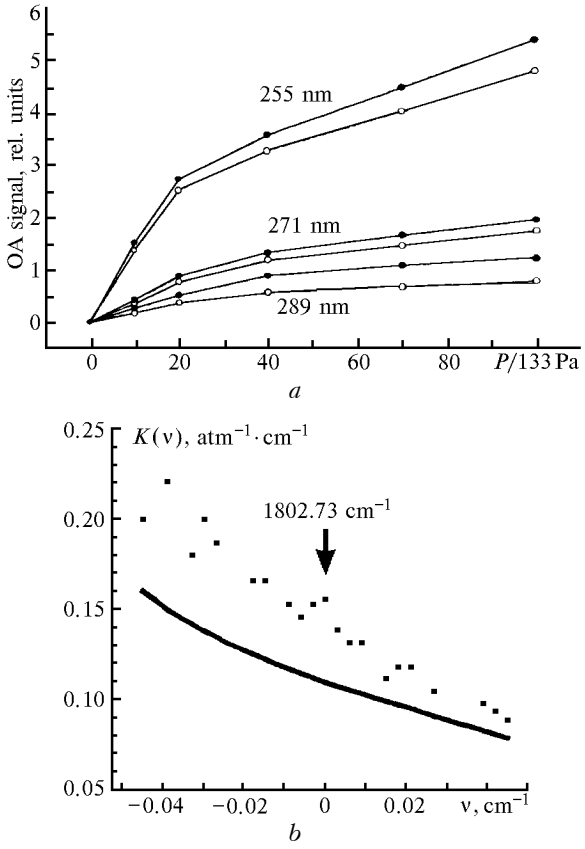

Fig. 4. Absorption of MVL radiation in the UV and IR spectral regions. Upper panel shows the opto-acoustic signal as a function of pressure (P, in Pa) in nitrogen and N_2–water mixture, λ = 255 and 289 nm are second harmonics of the Cu-vapor laser emission, and λ = 271 nm is the mixed radiation frequency; 100% N_2 (○), 92.5% N_2 + 7.5% H_2O (•). Lower panel shows the water vapor absorption coefficient at the Ca-vapor laser radiation frequencies, λ = 5.54 μm: calculations and measured results.

4. MVL's in determination of the atmospheric humidity

Water vapor is one of the principal and most variable atmospheric components. Its real-time monitoring can be provided for by the methods based on the resonance absorption of laser radiation, first of all, in the red and infrared spectral regions where the strongest absorption bands of H_2O lie.[19] MVL's can be efficient radiation sources for the corresponding devices measuring the air humidity. Among such MVL's are, in particular, Ca-vapor laser, λ = 5.54 μm, and Sr-vapor laser, λ = 6.45 μm. References 20–22 present the experimental results on water vapor absorption of radiation emitted by Ca- and Sr-vapor lasers. Dots in Fig. 4*b* show the experimentally obtained dependence[21] of the water vapor absorption coefficient $K(\nu)$, in $atm^{-1}\cdot cm^{-1}$, nearby 5.54 μm (with the frequency tuning by a magnetic field). The arrow indicates the Ca-vapor laser frequency in the absence of external magnetic field. The solid curve in this

figure shows the dependence $K(\nu)$ calculated by the dispersion formula for a single line centered at 1802.48 cm^{-1}. The data obtained in Refs. 20–22 are indicative of the possibility to construct the devices based on Ca- and Sr-vapor lasers for remote real-time monitoring of humidity in the atmosphere.

5. MVL's in the problems of radiative transfer through dense scattering media

The information about optical density of the scattering medium can be extracted not only from experiments on radiation extinction, but also in other ways, in particular, from deformation of an emitted short pulse.

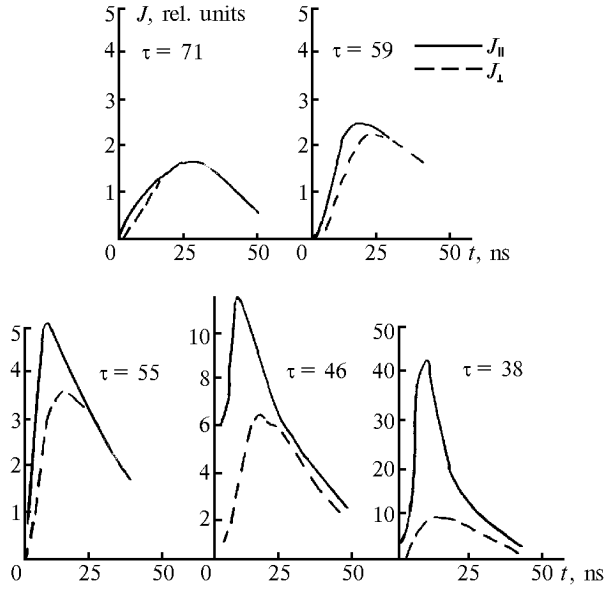

Fig. 5. Deformation of a pulse emitted by a Cu-vapor laser as it passes through dense scattering media (sounding pulse duration about 4 ns).

Figure 5 shows the time deformation of a short pulse at the green line of the copper-vapor laser as it passes through a model dense optical medium in the aerosol chamber.[23] The experiment was aimed at studying adiabatic fogs formed by throwing off the pressure in the chamber pressurized to an excess pressure of 1 atm. After completion of pressure throwing-off, the fog achieved its maximum density and then gradually degraded. Measurements were conducted during the period of fog degradation (about 20 min). The extinction coefficient of a fog was measured at different time using a He–Ne laser-based transmissometer at 0.63 μm along a short path (1 m). The accuracy of measurements of the optical depth τ, as converted to 20-m long path, was equal to ± 0.4. The duration of the sounding pulse was 4 ns at the time resolution of the recording system equal to 2 ns. The emitted (short) pulse experiences broadening in the optically dense medium due to multiple scattering. It follows from the obtained data that the quantitative characteristics of deformations of the emitted pulse caused by variations in the optical density of the sounded medium can be reliably obtained at the optical depth about 20 for the polarized component ($J_\parallel$) and about 10 for the cross polarized component ($J_\perp$).

6. MVL's in the problems of remote sounding of iodine radionuclides

Radioactive iodine isotopes are present in gaseous emissions from radiochemical plants, therefore development of methods for remote real-time monitoring of iodine in the atmosphere is an urgent problem. The analysis of spectroscopic properties of iodine molecules and copper-vapor laser radiation has shown that the copper-vapor laser transitions fall within the A, $B \leftarrow X$ band of the iodine molecule (Fig. 6*a*), while several lines of all the three iodine isotopes (127, 129, and 131) lie within the green and yellow lines of the Cu-vapor laser.

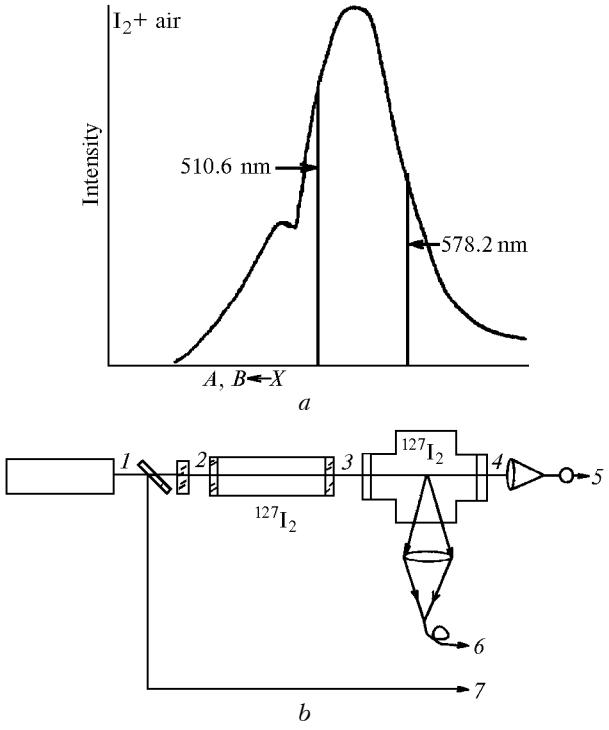

Fig. 6. Absorption of Cu-vapor laser radiation by iodine vapor: spectral position of the laser lines relative to the maximum of the A, $B \leftarrow X$ absorption band of I_2 (*a*); block diagram of the experimental setup (*b*).

In such a case, it becomes possible to develop a laser selective to every iodine isotope. To check this assumption, we have conducted experiments on selection of the Cu-vapor laser radiation by non-radioactive isotopic specie $^{127}I_2$ (Ref. 24). The

experimental setup (Fig. 6*b*) comprised a copper-vapor laser *1*, a set of filters *2* for separation of lines at 510.6 and 578.2 nm wavelengths in the laser radiation, an absorption cell with $^{127}I_2$ vapor *3*, and a fluorescence cell with the same vapor *4*. Correspondingly, two recording channels were used: the fluorescence channel *6* recording the intensity of fluorescence in the cell *4* and the absorption channel *5* for measuring the power of laser radiation upon its passage through the both cells, as well as the output power control channel *7*. At the first stage, iodine in the absorption cell was cooled, and signals in both channels were measured. Then the cell with iodine was heated up to ~ 40°C, and the changes in signals in both channels were recorded (Table 1).

Table 1

Wavelength, nm	Temperature inside the cell *3*, °C	Output power, rel. units	Intensity of fluorescence, rel. units
510.6	0	1	1
	40	0.25	0
578.2	0	1	1
	40	0.75	0

As could be expected, laser radiation is not fully absorbed, while no fluorescence is observed. This is indicative of deep selection of the Cu-vapor laser radiation by iodine $^{127}I_2$ vapor. Thus, we have the laser system selectively tuned to detection of radioactive iodine isotopic species. As this radiation is directed to a cell containing all the isotopic species of iodine, further extinction of radiation and fluorescence are caused by other (129 and 131) iodine isotopic species. The difference in absorption of the green and yellow lines of the copper-vapor laser is caused by the fact that $\lambda = 510.6$ nm is closer to the maximum of the iodine absorption band. The experiments on sounding the iodine vapor by fluorescence in typical emissions from radiochemical plants gave the following results (taking into account the factors of fluorescence quenching). At the mean output power of the selected radiation $\gtrsim 1$ W, the sounding range of 1000 m, the layer depth of 10 m, and the receiving mirror area of 0.25 m^2, the received signal is above 1 photon/s, what is quite acceptable for the current recording systems. Taking into account that the copper-vapor laser is the best source of high-power coherent radiation operating in the $A, b \rightarrow u$ iodine absorption band, the possibility using it in lidar systems for monitoring of iodine radionuclides seems to be rather realistic.

7. Detection and ranging of metal layers in the upper atmosphere

Characteristic gaseous components of the upper atmosphere and near space include atoms and ions of chemical elements in the ground, metastable, and ionized states.[25] They play an important part in physicochemical reactions and radiative properties of the upper atmosphere. The presence of atoms and ions in the upper atmosphere is caused not only by meteor material, but also by vertical transfer from the Earth's surface. The question, which mechanism is governing, is now under discussion. The densities of minor constituents, their altitude profiles, and other parameters are now practically unstudied (except for Ca and Na vapors[26,27]). In Ref. 28 a simple scheme proposed by Klimkin was analyzed for detection of metastable atoms in the upper atmosphere from the ground and from space. A hypothetical layer of copper atoms at the altitude about 90 km was taken as a test object. This choice can be explained by the following reasoning. First, copper is an element of medium abundance in both meteor and Earth's sources. Second, for sounding of the copper layers we have the most powerful metal vapor laser, namely, copper-vapor laser.[29–32] Third, for copper atoms both exciting radiation and the fluorescence (informative channel) are weakly absorbed by atmospheric gases. Fourth, the layers of minor constituents are situated, as a rule, at the altitudes between 80 and 100 km (Ref. 25). The principal scheme of excitation of the anti-Stokes fluorescence in the high-altitude layer of copper atoms containing metastable atoms is shown in Fig. 7.

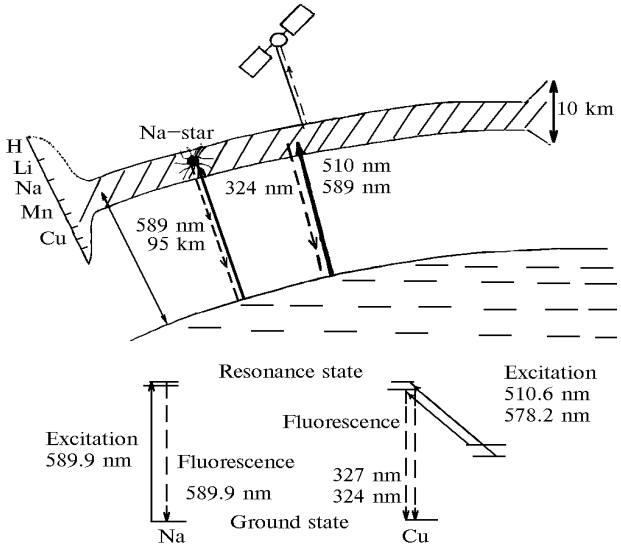

Fig. 7. Scheme for detecting high-altitude layers of metal atoms. The lower panel shows a simplified scheme of transitions.

It is assumed that initially some atoms are in the excited metastable states $^2D_{3/2,5/2}$ (this assumption is justified because in the upper atmosphere we deal with a weakly ionized plasma). Under exposure to Cu-vapor laser radiation (excitation channel) some metastable atoms transit to the resonance states $^2P_{1/2,3/2}$ with the following emission at resonance transitions into the ground ($^2S_{1/2}$) state (fluorescence channel). The

model calculations have shown that use of a copper-vapor laser with typical output parameters (mean output power of 10 W at the pulse repetition rate of 10 kHz and pulse duration of 20 ns) and the receiving telescope with the mirror diameter of 1 m would provide for the photon count rate in the fluorescence channel that could be quite acceptable (1 photon/s) for realistic measurements. This method is suitable for detection of other elements along with the copper atoms. If the atmosphere is transparent for the both of excitation and fluorescence channels, ground-based sounding is possible (atoms of bismuth and thulium, ions of calcium and barium). If the atmosphere is not transparent for at least one channel, then sounding can be carried out from on board a spacecraft orbiting at the altitude of 300 km. In this case, besides the above-listed elements, the fluorescent method is capable of detecting the atoms of manganese, strontium, Au, Pb, calcium, and europium, as well as ions of strontium and europium.

8. MVL's in visual navigation systems

A large number of laser navigation systems (LNS's) are now known, which are intended for solution of the problems associated with orientation of moving objects in space under conditions of limited visibility. The operation of LNS's is based on the fact that the contrast between the brightness of the direct radiation carrying information on the source position and the background of scattered radiation for narrow laser beams is observed at distances far exceeding those for the case of point-like or weakly collimated radiation sources, such as traditional navigation lights.[33] Among navigation systems, rotating laser beacons of circular, sectorial, and transit types have gained the widest acceptance.[34] Circular beacons provide for the light to be visible from any direction. Sectorial and transit beacons as a warning beacons are used to mark dangerous and safe places. The operating principle of a sectorial beacon using three laser beams of different color (red, yellow, and green) is explained by the scheme given in Fig. 8. The angular sizes of the orientation zones swept out by the horizontal and vertical scanning devices can be changed from 15 min. of arc to 5° in the vertical plane and from 15 min. of arc to 12° in the horizontal plane. So, this beacon can be used as both the sectorial and transit one. In Ref. 35 the copper-aurum vapor laser operating at 510.6, 578.2, and 627.8 nm was used as a radiation source for such a beacon. Since the laser operates in the repetitively pulsed mode with pulse duration of 20 to 30 ns and the gap between pulses of tens microseconds, dark spots may appear in the color sectors while scanning.

Let us estimate the required laser pulse repetition rate. First, consider the case of continuous radiation scanning. The scanning frequency in the vertical plane in the presence of horizontal sweep within the angle β can be determined as

$$F = K\,\beta/(\alpha\, t), \tag{3}$$

where α is the total beam divergence; t is the frame fill time; K is the coefficient allowing for the beam stop which is needed for complete frame fill (see Fig. 6*b*) $1 < K < 2$. Then for typical values $\beta = 2 - 4°$ (for calculation we took the maximum value), $\alpha = 5$ min, $t = 1$ s, and $K = 2$ we have $F = 96$ Hz.

Now take into account that radiation is of repetitively pulsed character with the pulse duration $\tau \sim 10^{-8}$ s. The time during which the beam propagates from x_1 to x_n is:

$$t_n = 1/2F \sim 5\cdot 10^{-3}\ \text{s}. \tag{4}$$

Since $\tau \ll t_n$, the solid angle $\alpha = 5$ min occupied by a beam from a single pulse remains almost unchanged during scanning. Let N be the number of flashes as the beam propagates from x_1 to x_n:

$$N = \gamma/\alpha, \tag{5}$$

where γ is the vertical sweep angle.

Taking into account the requirement of the maximum frame fill

$$N = K\,\gamma/\alpha. \tag{6}$$

Then

$$T/2 = t_n/N, \tag{7}$$

where $T = 1/f_n$ is the period, f_n is the minimum pulse repetition frequency of an MVL, which provides for complete frame fill. For the maximum angular size in the vertical plane $\gamma = 5°$ we have

$$f_n = K\,\gamma/2t\,\alpha = 12\ \text{kHz}. \tag{8}$$

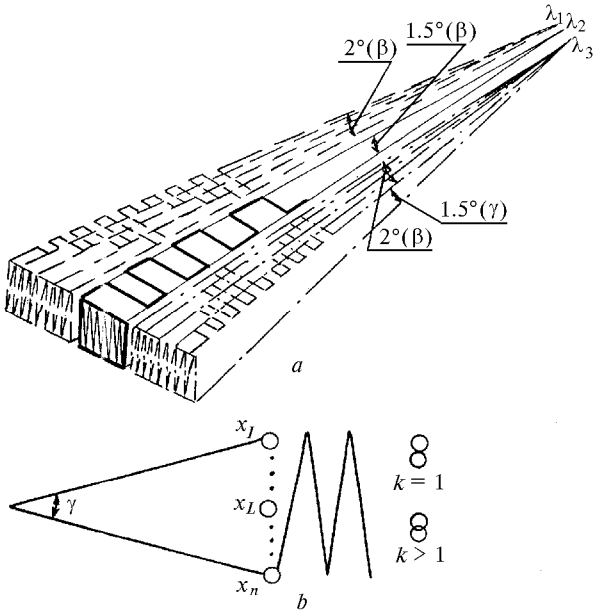

Fig. 8. Operating principle of a laser navigation device with a three-color repetitively pulsed emitter: the scheme of sector formation (*a*); scheme explaining the frame fill (*b*).

Thus, the pulse repetition rate of the MVL used as a radiation source in a beacon should be higher than 12 kHz. The scanning frequency in the horizontal plane

is about several Hz, and, correspondingly, the requirements imposed on the pulse repetition rate are met with a safety margin. (The pulse repetition rate required for laser devices used for airplane landing is 100 kHz and higher.) The required mean output power depending on the fog density does not exceed 1 W, and the beacon operation range in this case is from several kilometers to tens of kilometers. Other requirements imposed on radiation sources for LNS's are: beam divergence about several minutes of arc, strict stability of the axis of the directional pattern, small size and low energy consumption, capability of operating in unattended mode in not specially equipped rooms under conditions of high humidity and large temperature differences. In accordance with these requirements, Milan–02 and Milan–SM copper and Au vapor lasers were manufactured at the Institute of Atmospheric Optics in cooperation with the Design Office BOptikaB to operate as radiation sources of Raduga and Liman laser navigation systems.[36] The Raduga navigation system has passed one-year test operation in Ventspils sea port. It provided for ship transit through a narrow approach channel 11.4 km long and 130 m wide under conditions of limited visibility.

9. MVL's in atmospheric adaptive optics devices

Another interesting application of the MVL's at present days and in the future is creation of artificial reference stars for adaptive optical systems, in particular, for obtaining high-quality images of planets, actual stars, etc. In this applications, as in the above-considered ones, the copper-vapor laser, which is the most efficient laser in the visible spectral range, has practically no competitors. To BstartB an artificial reference star, the Rayleigh scattering of the Cu-vapor laser radiation focused at the altitude H = 10–15 km or excitation of fluorescence in the high-altitude sodium layers (H = 90 km) by a copper-vapor-laser-pumped dye laser tuned to sodium D-lines is used.[37,38] A laser system is, as a rule, built in the transceiving part of a ground-based adaptive telescope. In particular, Ref. 37 considers the adaptive system with 1.5-m mirror (USA). As a radiation source, it utilizes the system of several copper-vapor lasers manufactured at Oxford Lasers Ltd. Besides, it includes the master oscillator based on 40-W laser with injection generating a quality beam and three amplifiers based on one 40-W laser and two 100-W lasers. This system provides for emission of the radiation beam with the mean output power of 60–70 W (taking into account the power losses at the elements of the optical system) and divergence close to the diffraction one at the pulse repetition rate of 5 kHz. Technical capabilities of the telescope with correction against an artificial reference star are illustrated by Fig. 9 borrowed from Ref. 37. This figure shows the photographs of Saturn taken with an ordinary telescope and with an adaptive optics system using correction against an artificial reference star.

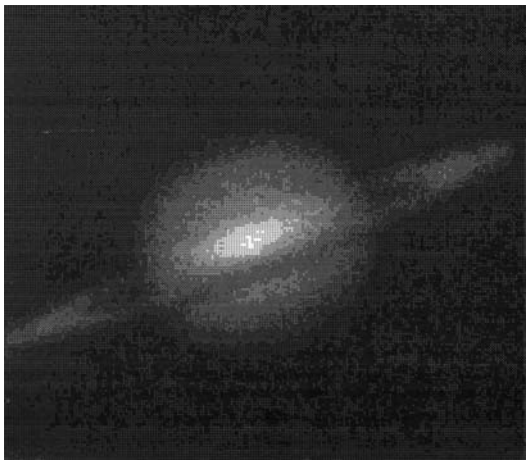

a

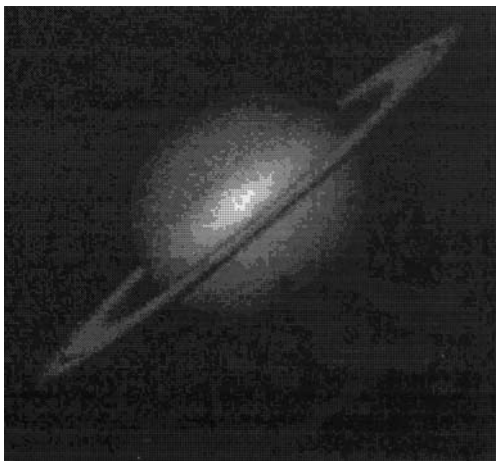

b

Fig. 9. Saturn images taken with an ordinary telescope (*a*) and with an adaptive optical system employing correction against an artificial reference star (*b*).

10. MVL's in side view lidars

The most promising application of MVL's in atmospheric optics and hydrooptics is their use in side view lidars. These promises are caused by high repetition rate of laser pulses which allows the spatial raster to be obtained with good resolution, for example, 100×100 pixels at a frame frequency of 1 to 10 Hz. In the atmosphere such a lidar provides the ability to solve a unique problem of visualization of otherwise invisible aerosol and gas formations. The objects of visualization in hydrooptics may be hydrosol formations, thermal ridges, waters contacts, small objects.

A Cu-vapor-laser-based device providing stable spatial raster has been designed at the Institute of Atmospheric Optics. The block-diagram of this device is shown in Fig. 10.

The 200×60 raster was scanned with the help of the mirror optical–mechanical system. The laser was initiated by synchropulses formed by a computer. Line and frame synchropulses were generated by a specialized optical scheme of the scanning unit. In relatively simple problems, such as visualization of an

aerosol formation, an image can be formed with the sounding range of 1 to 2 km at the resolution of 20 m.

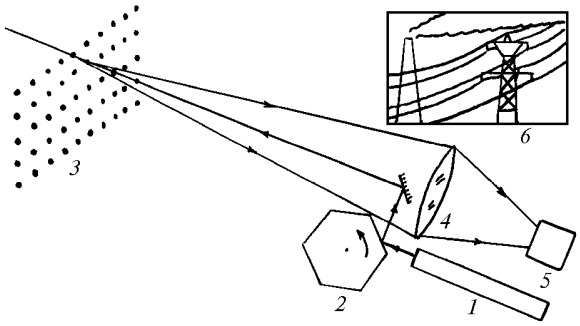

Fig. 10. "lock diagram of the side view lidar: Cu-vapor laser (*1*); unit for optical–mechanical scanning (*2*); spatial raster (*3*); objective (*4*); photodetector (*5*); a fragment of industrial landscape at the lidar display (*6*).

11. Conclusion

Certainly, the examples presented in this paper do not exhaust the complete list of MVL applications in atmospheric optics. In particular, high-power MVL's with high repetition rate (more than 100 kHz) can be used to detect objects moving in the atmosphere, to create light-dynamic effects on natural and artificial clouds, etc.

The above material confirms the fact that already in the near future atmospheric optics can become an area of efficient application of metal vapor lasers.

References

1. G.S. Evtushenko, in: *Pulsed Metal Vapor Lasers: Proceedings of the NATO Advanced Research Workshop on Pulsed Metal Vapor Lasers – Physics and Emerging Applications in Industry, Medicine, and Science*, ed. by C.E. Little and N.V. Sabotinov. NATO ASI Series, 1. Disarmament Technologies Vol. 5. (Kluwer Academic Publishers, 1995), pp. 445–452.
2. V.E. Zuev, *Laser as a Meteorologist* (Gidrometeoizdat, Leningrad, 1974), 179 pp.
3. A.N. Tikhonov and V.Ya. Arsenin, *Methods for Solution of Ill-Posed Problems* (Nauka, Moscow, 1974), 223 pp.
4. V.E. Zuev and V.V. Zuev, *Remote Optical Sensing of the Atmosphere* (Gidrometeoizdat, St. Petersburg, 1992), 232 pp.
5. I.E. Naats, *Theory of Multifrequency Laser Sounding of the Atmosphere* (Nauka, Novosibirsk, 1980), 157 pp.
6. I.E. Naats, *Method of Inverse Problem in Atmospheric Optics* (Nauka, Novosibirsk, 1986), 198 pp.
7. Yu.F. Arshinov, S.M. Bobrovnikov, V.E. Zuev, and V.M. Mitev, Appl. Opt. **22**, No. 19, 2984–2990 (1983).
8. Yu.F. Arshinov, S.M. Bobrovnikov, V.K. Shumskii, et al., Atmos. Oceanic Opt. **5**, No. 7, 459–461 (1992).
9. Yu.F. Arshinov, S.M. Bobrovnikov, I.B. Serikov, et al., Atmos. Oceanic Opt. **10**, No. 3, 221–224 (1997).
10. V.D. Burlakov, V.V. Zuev, G.S. Evtushenko, et al., Atmos. Oceanic Opt. **6**, No. 3, 204–207 (1993).
11. D.V. Stoyanov, A.K. Donchev, Zh.V. Kolarov, and A. Mitsev, Opt. Atm. **1**, No. 4, 109–116 (1988).
12. V.D. Burlakov, V.V. Zuev, G.S. Evtushenko, et al., Atmos. Oceanic Opt. **7**, Nos. 11–12, 876–879 (1994).
13. V.D. Burlakov, V.V. Zuev, G.S. Evtushenko, et al., in: Proc. SPIE. Atomic and Molecular Pulsed Lasers **2619**, 270–275 (1995).
14. Yu.F. Arshinov, V.E. Zuev, I.E. Naats, et al., in: *Proc. Intern. Conf. on Lasers'82*, New Orleans, Louisiana (STS Press. Mc. Lean, 1982).
15. B.A. Tikhomirov, V.O. Troitskii, V.A. Kapitanov, et al., Acta Physica Sinica **7**, No. 3, 190–195 (1998).
16. V.M. Klimkin and V.N. Fedorishchev, Atm. Opt. **2**, No. 2, 174–175 (1989).
17. S.F. Luk'yanenko, T.I. Novokovskaya, and I.N. Potapkin, Atm. Opt. **3**, No. 11, 1080–1082 (1990).
18. Yu.N. Ponomarev and I.S. Tyryshkin, Atmos. Oceanic Opt. **6**, No. 4, 224–228 (1993).
19. V. Eppers, in: *Handbook on Lasers*, ed. by A.M. Prokhorov (Sov. Radio, Moscow, 1978), Vol. 1, pp. 380–465.
20. V.M. Klimkin and P.D. Kolbycheva, in: P*roceedings of the All-Union SymPosium on Laser Radiation ProPagation through the Atmosphere* (Institute of Atmospheric Optics Publishing House, Tomsk, 1977), pp. 12–14.
21. V.M. Klimkin and P.D. Kolbycheva, Atmos. Oceanic Opt. **11**, No. 9, 841–844 (1998).
22. V.N. Marichev, A.V. Platonov, A.N. Soldatov, et al., in: *Measuring Devices for Studying Parameters of the Surface Atmospheric Layers* (Institute of Atmospheric Optics Publishing House, Tomsk, 1977), pp. 80–86.
23. V.V. Vergun, A.E. Kirilov, G.P. Kokhanenko, et al., Dep. v VINITI, No. 2568–b 86 (1986), 18 pp.
24. L.P. Vorob'eva, G.S. Evtushenko, V.M. Klimkin, et al., Atmos. Oceanic Opt. **8**, No. 11, 908–910 (1995).
25. *Atmosphere. Handbook* (Gidrometeoizdat, Leningrad, 1991), 509 pp.
26. E.D. Hinkley, ed., *Laser Monitoring of the Atmosphere* (Springer Verlag, New York, 1976).
27. R.M. Measures, *Laser Remote Sensing* (Wiley&Sons, New York, 1987).
28. G.S. Evtushenko, M.Yu. Kataev, and V.M. Klimkin, Atmos. Oceanic Opt. **9**, No. 8, 730–733 (1996).
29. G.G. Petrash, Usp. Fiz. Nauk **105**, No. 4, 645–676 (1971).
30. A.N. Soldatov and V.I. Solomonov, *Gas Discharge Lasers at Self-Limited Transitions in Metal Vapor* (Nauka, Novosibirsk, 1985), 152 pp.
31. V.M. Batenin, V.V. Buchanov, M.A. Kazaryan, I.I. Klimovskii, and E.I. Molodykh, *Lasers at Self-Limited Transitions of Metal Atoms* (RFFI, Moscow, 1998), 544 pp.
32. C.E. Little, *Metal Vapor Lasers: Physics, Engineering & Applications* (Wiley&Sons, Chichester, UK, 1998), 620 pp.
33. V.E. Zuev and M.V. Kabanov, *Optical Signal Transfer in the Earth's Atmosphere (under Noise Conditions)* (Sov. Radio, Moscow, 1977), 368 pp.
34. V.E. Zuev and V.Ya. Fadeev, *Laser Navigation Systems* (Radio i Svyaz', Moscow, 1987), 161 pp.
35. G.S. Evtushenko, A.N. Soldatov, Yu.P. Polunin, et al., Zh. Prikl. Spektrosk. **39**, No. 6, 939–944 (1983).
36. G.S. Evtushenko, V.Yu. Kashaev, V.V. Tatur, et al., in: *Abstracts of Reports at the Third All-Union Conference on Application of Lasers in Technology and Information Transfer and Processing Systems*, Tallinn (1988), Part 2, pp. 94–95.
37. R.Q. Fugate, in: *Pulsed Metal Vapor Lasers. Proceedings of the NATO Advanced Research Workshop on Pulsed Metal Vapor Lasers – Physic and Emerging Applications in Industry, Medicine and Science*, ed. by C.E. Little and N.V. Sabotinov. NATO ASI Series, 1. Disarmament Technologies V. 5 (Kluwer Academic Publishers, 1995), pp. 431–440.
38. R.A. Humphreys, L.E. Bradley, and J. Herrmann, Lincoln Laboratory Journal **5**, No. 1, 45–65 (1992).